

OPTIMAL AND LOW-MEMORY NEAR-OPTIMAL PRECONDITIONING OF FULLY IMPLICIT RUNGE-KUTTA SCHEMES FOR PARABOLIC PDES

XIANGMIN JIAO^{*†}, XUEBIN WANG^{*}, AND QIAO CHEN^{*}

Abstract. Runge-Kutta (RK) schemes, especially Gauss-Legendre and some other fully implicit RK (FIRK) schemes, are desirable for the time integration of parabolic partial differential equations due to their A-stability and high-order accuracy. However, it is significantly more challenging to construct optimal preconditioners for them compared to semi-implicit RK (aka diagonally implicit RK or DIRK) schemes. To address this challenge, we first introduce mathematically optimal preconditioners called *block complex Schur decomposition (BCSD)*, *block real Schur decomposition (BRSD)*, and *block Jordan form (BJF)*, motivated by block-circulant preconditioners and Jordan form solution techniques for IRK. We then derive an efficient, near-optimal *singly-diagonal approximate BRSD (SABRS)* by approximating the quasi-triangular matrix in real Schur decomposition using an optimized upper-triangular matrix with a single diagonal value. A desirable feature of SABRS is that it has comparable memory requirements and factorization cost as singly DIRK (SDIRK). We approximately factorize the diagonal blocks in these preconditioners using a near-linear-complexity multilevel ILU factorization called HILUCSI, which is significantly more robust and more efficient than ILU(0). We apply the preconditioners in right-preconditioned GMRES to solve the advection-diffusion equation in 3D using finite element and finite difference methods. We show that BCSD, BRSD, and BJF significantly outperform other preconditioners in terms of GMRES iterations, and SABRS is competitive with them and the prior state of the art in terms of computational cost while requiring the least amount of memory.

Key words. fully implicit Runge-Kutta; Gauss-Legendre schemes; preconditioning; block Schur decomposition; low-memory requirement; multilevel ILU; parabolic partial differential equations

AMS subject classifications. 65F08, 65F50, 65M99

1. Introduction. We consider the solution of time-dependent parabolic partial differential equations (PDEs), such as the advection-diffusion (AD) equation for $u : \Omega \times [0, T] \rightarrow \mathbb{R}$,

$$(1.1) \quad u_t - \nabla \cdot (\mu \nabla u) + \mathbf{v} \cdot \nabla u = f,$$

where $\mu \geq 0$ denotes the diffusion coefficient, \mathbf{v} denotes a velocity field, f denotes some source term, and u_t denotes the temporal derivative. In the extreme case of $\mathbf{v} = \mathbf{0}$, (1.1) reduces to the heat equation. Typically, the spatial discretization uses finite difference methods (FDM) or finite element methods (FEM). We assume the spatial discretization is well-posed, and (1.1) is diffusion dominant in the sense that the mesh Péclet number $\text{Pe}_h = 2h\|\mathbf{v}\|/\mu \lesssim 1$ [20], where h denotes a characteristic edge length of the mesh.

These methods convert (1.1) into a system of stiff ordinary differential equations (ODEs),

$$(1.2) \quad \mathbf{M}u_t(t) = -\mathbf{K}u(t) + \mathbf{f}(t),$$

where $\mathbf{M} \in \mathbb{R}^{m \times m}$ and $\mathbf{K} \in \mathbb{R}^{m \times m}$ denote the mass and stiffness matrices (see Section 2.2), correspondingly, and $\mathbf{f} : [0, T] \rightarrow \mathbb{R}^m$. For long-time integration, fourth and higher-order accurate FDM and FEM (including spectral elements [30]) are often used. Therefore, it is desirable to solve (1.2) using high-order implicit time-integration schemes that are A-stable, so that large time steps can be used without compromising stability and accuracy.

The Gauss-Legendre, Radau IIA, Lobatto IIIC, and some other implicit Runge-Kutta (IRK) are attractive for their A-stability and high-order accuracy; see, e.g., [10, 23, 25]. An s -stage Runge-Kutta (RK) scheme can be expressed by the Butcher tableau $\begin{array}{c|c} \mathbf{c} & \mathbf{A} \\ \hline & \mathbf{b}^T \end{array}$ [10],

^{*}Department of Applied Mathematics & Statistics and Institute for Advanced Computational Science, Stony Brook University, Stony Brook, NY 11794, USA.

[†]Corresponding author. Email: xiangmin.jiao@stonybrook.edu.

where $\mathbf{A} \in \mathbb{R}^{s \times s}$, $\mathbf{c} \in \mathbb{R}^s$, and $\mathbf{b} \in \mathbb{R}^s$. For A-stable IRK schemes with an invertible \mathbf{A} , the real part of the eigenvalues of \mathbf{A} are all positive [23, p. 402]. Given an s -stage IRK and time step δt , (1.2) leads to an $sm \times sm$ linear system $\mathcal{A}\mathcal{U} = \mathcal{B}$ with

$$(1.3) \quad \mathcal{A} = \mathbf{I}_s \otimes \mathbf{M} + \delta t \mathbf{A} \otimes \mathbf{K},$$

where \mathbf{I}_s is the $s \times s$ identity matrix, \otimes denotes the Kronecker-product operator, and \mathcal{B} depends on the solution in the previous time step, the boundary conditions, and the source term \mathbf{f} ; see, e.g., [18, p. 223]. Unless otherwise noted, we use boldface and regular calligraphic fonts to indicate block matrices and vectors, respectively. Let b_i denote the entries in \mathbf{b} and $\mathbf{k}_i \in \mathbb{R}^m$ denote the subvectors in \mathcal{U} corresponding to stage i for $i = 1, 2, \dots, s$. The solution at time step $k + 1$ is then $\mathbf{u}_{k+1} = \mathbf{u}_k + \delta t \sum_{i=1}^s b_i \mathbf{k}_i$. We aim to construct a *right preconditioner* $\mathcal{M} \in \mathbb{R}^{sm \times sm}$ and to solve the preconditioned system

$$(1.4) \quad \mathcal{A}\mathcal{M}^{-1}\mathcal{V} = \mathcal{B}$$

using a Krylov-subspace (KSP) method (such as GMRES [43]), and then $\mathcal{U} = \mathcal{M}^{-1}\mathcal{V}$.

Among the IRK schemes, the fully implicit RK (FIRK) schemes have the highest-order accuracy. In particular, the s -stage Gauss-Legendre (GL) [25] (aka Gauss [23]) are of order $2s$. However, the Butcher matrix \mathbf{A} for FIRK is typically full, so it is more challenging to construct effective and robust preconditioners for them compared to semi-implicit RK (aka diagonally implicit Runge-Kutta or DIRK) schemes [35], for which \mathbf{A} and \mathcal{A} are lower triangular and block lower triangular, respectively. Among the DIRK schemes, singly DIRK (SDIRK) [23, IV.6] are often used, because the diagonal entries in \mathbf{A} are all equal and in turn they lead to lower factorization cost and memory requirement. However, an s -stage SDIRK is limited to order- $(s + 1)$, which is far lower than an s -stage GL for large s . Hence, there are significant interests in developing effective preconditioners for FIRK; see, e.g., [13, 26, 36, 44, 48]. Those preconditioners typically have a similar cost as DIRK or SDIRK per iteration, but the number of KSP iterations may be far from optimal.

In this work, we introduce optimal and limited-memory near-optimal preconditioners for FIRK. Our approach is novel in two main aspects. First, we introduce three block-preconditioners called BCSD, BRSD, and BJF, based on the complex and real Schur decompositions and the Jordan decomposition, respectively. These preconditioners are motivated by block circulant preconditioners [11] and the Jordan form solution techniques for IRK [5, 9], and they are mathematically optimal in exact arithmetic. Second, we introduce a *singly-diagonal approximate BRSD* (SABRS) preconditioner, which reduces the memory requirement and the factorization times compared to the aforementioned optimal preconditioners. We approximately factorize the diagonal blocks in these block preconditioners using a near-linear-complexity multilevel ILU technique called HILUCSI [15], which is significantly more robust and more efficient than the commonly used ILU(0) [29, 36, 37] on finer meshes. Our experimental results show that BCSD, BRSD, and BJF significantly outperform other preconditioners in terms of the number of GMRES iterations. SABRS compares favorably to the prior state of the art in terms of computational cost while requiring the least amount of memory.

The remainder of the paper is organized as follows. In Section 2, we review some background on FDM and FEM, optimal preconditioning, and some existing preconditioners for FIRK. In Section 3, we introduce the mathematically optimal BCSD, BRSD, and BJF. In Section 4, we introduce the near-optimal SABRS preconditioners based on BRSD by deriving a novel optimization strategy. In Section 5, we present numerical results with the proposed preconditioners, verify their (near) optimality, and compare them with the prior state-of-the-art preconditioners. Finally, Section 6 concludes the paper with a brief discussion of future research directions.

2. Preliminaries and Related Works. We start by reviewing some basics of preconditioning techniques, especially in the context of FIRK.

2.1. Optimal preconditioning. Our aim in this work is to develop optimal and near-optimal right preconditioners that are stable, accurate, and efficient for FIRK. We prefer right preconditioning in that it does not affect the norm of the residual vector, which is preferable for GMRES [21]. To measure the stability and accuracy of preconditioners, we use a definition based on that in [27], which generalized some other measures reviewed in [3].

DEFINITION 2.1. *Given $\mathcal{A} \in \mathbb{R}^{n \times n}$, \mathcal{G} is an ϵ -accurate right-preconditioning operator (RPO) for \mathcal{A} if there exists a nonsingular $\mathcal{X} \in \mathbb{R}^{n \times n}$ (or $\in \mathbb{C}^{n \times n}$) such that*

$$(2.1) \quad \left\| \mathcal{X}^{-1} (\mathcal{A}\mathcal{G}) \mathcal{X} - \begin{bmatrix} \mathbf{I}_r & \\ & \mathbf{0} \end{bmatrix} \right\| = \epsilon < 1,$$

where $r = \text{rank}(\mathcal{A})$. A class of RPO is ϵ -accurate if ϵ tends to 0 as its control parameters are tightened. \mathcal{G} is stable if $\kappa(\mathcal{X}) \leq C$ for some bounded $C > 1$. An ϵ -accurate RPO is mathematically optimal if $\epsilon = 0$.

Definition 2.1 is general in that it applies to both singular and nonsingular systems. For nonsingular matrices, which are the focus of this work, the reader can simply interpret $\mathcal{G} = \mathcal{M}^{-1}$ for a nonsingular $\mathcal{M} \in \mathbb{R}^{n \times n}$ (or $\in \mathbb{C}^{n \times n}$), where \mathcal{M} is the *right preconditioner*, and \mathcal{G} is mathematically optimal if and only if $\mathcal{M} = \mathcal{A}$. More generally, however, \mathcal{G} does not need to be the inverse of a nonsingular matrix [27]; in this case, an ϵ -accurate RPO guarantees the breakdown-free of GMRES for consistent systems [27, Theorem 3.9]. More intuitively, since $\left\| \mathcal{X}^{-1} (\mathcal{A}\mathcal{M}^{-1}) \mathcal{X} - \mathbf{I} \right\| \leq \kappa(\mathcal{X}) \|\mathcal{M}^{-1}\| \|\mathcal{A} - \mathcal{M}\|$, ϵ -accuracy for nonsingular matrices depends on how close \mathcal{M} is to \mathcal{A} and how well conditioned \mathcal{X} and \mathcal{M} are in (2.1). For this reason, Definition 2.1 is useful in assessing preconditioners qualitatively. In addition, we will also use Definition 2.1 to derive objective functions in optimizing \mathcal{M} quantitatively.

Efficiency is multifaceted, including the factorization of \mathcal{M} , the solve $\mathcal{M}^{-1}\mathcal{V}$, the number of KSP iterations, the sparse matrix-vector (SpMV) multiplication $\mathcal{A}\mathcal{U}$, and the memory requirement. From a practical point of view, we use the following criterion, assuming that the solve time of $\mathcal{M}^{-1}\mathcal{V}$ dominates that of SpMV $\mathcal{A}\mathcal{U}$.

DEFINITION 2.2. *A preconditioner \mathcal{M} is near-optimal if it is ϵ -accurate and it takes (near) linear time to factorize and solve (per KSP iteration).*

In the context of IRK, the preconditioner \mathcal{M} can be reused if the mesh and δt remain the same. Hence, the factorization time can be amortized over many time steps. However, the memory requirement and the solve time for $\mathcal{M}^{-1}\mathcal{V}$ must be (near) linear. Of course, (near) linear time is impractical in Definition 2.2 for $\epsilon = 0$, so our goal is to make ϵ as small as possible.

2.2. Mass and stiffness matrices from FEM and FDM. Let us first briefly review the finite element methods (FEM). Given $\Omega \in \mathbb{R}^d$ with a piecewise smooth boundary, a set of trial (basis) functions $\{\phi_j(\mathbf{x}) : \Omega \rightarrow \mathbb{R} \mid 1 \leq j \leq m\}$ and a set of test functions $\{\psi_i(\mathbf{x}) : \Omega \rightarrow \mathbb{R} \mid 1 \leq i \leq m\}$, an FEM (or a *weighted-residual method*) approximates the continuum solution u by $\sum_{j=1}^m U_j \phi_j(\mathbf{x})$ and requires the residual to be orthogonal to $\{\psi_i\}$. After applying integration by parts, (1.1) is converted into a system of ODEs (1.2), where

$$(2.2) \quad \mathbf{M}_{\text{FEM}} = \left[\int_{\Omega} \phi_j \psi_i \, d\mathbf{x} \right]_{ij} \quad \text{and} \quad \mathbf{K}_{\text{FEM}} = \left[\int_{\Omega} \mu \nabla \phi_j \cdot \nabla \psi_i + (\mathbf{v} \cdot \nabla \phi_j) \psi_i \, d\mathbf{x} \right]_{ij}.$$

In the Galerkin FEM, $\{\phi_j\} = \{\psi_i\}$. \mathbf{M}_{FEM} is called the *mass matrix*, and \mathbf{K}_{FEM} is called the *stiffness matrix* when $\mathbf{v} = \mathbf{0}$.

A FDM is a collocation method, which we can interpret as a *generalized weighted residual method* [16], where the “test functions” are the Dirac delta functions at the nodes. The finite difference formula at the i th node can be constructed from a corresponding set of local basis functions $\{\phi_{ij}(\mathbf{x}) : \Omega \rightarrow \mathbb{R} \mid 1 \leq i, j \leq m\}$. We then have

$$(2.3) \quad \mathbf{M}_{\text{FDM}} = \mathbf{I} \quad \text{and} \quad \mathbf{K}_{\text{FDM}} = [-\nabla \cdot (\mu \nabla \phi_{ij}) + \mathbf{v} \cdot \nabla \phi_{ij}]_{ij}.$$

For convenience, we also refer to \mathbf{M}_{FDM} as the mass matrix in FDM, and we informally refer to both \mathbf{K}_{FEM} and \mathbf{K}_{FDM} also as the “stiffness” matrix even when $\mathbf{v} \neq \mathbf{0}$. For simplicity, we will omit their subscript when there is no confusion. Assuming $\mu > 0$ and well-posedness of the spatial discretization, \mathbf{K} for FEM is positive definite in that $\mathbf{K} + \mathbf{K}^T$ is symmetric and positive definite (SPD). For Galerkin FEM, \mathbf{M} is SPD with a Cholesky factorization $\mathbf{M} = \mathbf{R}^T \mathbf{R}$. Hence, $\mathbf{M}^{-1} \mathbf{K}$ is also positive definite for its similarity with $\mathbf{R}^{-T} \mathbf{K} \mathbf{R}^{-1}$, which has the same inertia as \mathbf{K} [22, p. 448]. For FDM, $\mathbf{M}^{-1} \mathbf{K} = \mathbf{K}$, which is also positive definite on sufficiently fine meshes [28].

The preceding spatial discretizations lead to a system of ODEs, which is stiff because $\kappa(\mathbf{K}) = \mathcal{O}(h^{-2})$ and $\kappa(\mathbf{M}) = \mathcal{O}(1)$ for both FEM on quasiuniform mesh [20] and FDM on uniform mesh [31], where h denotes some characteristic edge length of the mesh. Due to the positive definiteness of $\mathbf{M}^{-1} \mathbf{K}$, an A-stable IRK ensures an accurate and stable solution of (1.2). An IRK scheme leads to a linear system with the coefficient matrix (1.3). Let a_{ij} denote the entries in the Butcher matrix \mathbf{A} . If \mathbf{A} has positive diagonal entries a_{ii} , each diagonal block of \mathcal{A} has the form $\mathbf{M} + a_{ii} \delta t \mathbf{K}$, which is also positive definite.

When preconditioning FIRK, the fundamental question is how to express an approximate inverse of \mathcal{A} in terms of the approximate factorization of linear combinations of \mathbf{M} and \mathbf{K} as in (1.3). The following relationship between the stiffness and mass matrices will turn out to be useful in analyzing existing preconditioners.

LEMMA 2.3. *For diffusion-dominated AD equations, $\|\mathbf{K}\| = \mathcal{O}(h^{-2})\|\mathbf{M}\|$ for well-posed FEM and FDM.*

We omit the proof; see, e.g., [20] for FEM and [16] for a unified analysis of FEM and FDM. Lemma 2.3 leads to the following proposition.

PROPOSITION 2.4. *For diffusion-dominated AD equations, $\delta t \mathbf{A} \otimes \mathbf{K}$ and $\mathbf{I}_s \otimes \mathbf{M}$ converge to mathematically optimal preconditioners as $h^{-2} \delta t$ tends to ∞ and 0, respectively.*

Proof. As $h^{-2} \delta t$ tends to ∞ and 0, \mathbf{M} and \mathbf{K} in (1.3) can be omitted, respectively. \square

In general, $\delta t \gtrsim \mathcal{O}(h)$ when using implicit schemes, and hence the limiting case of $h^{-2} \delta t \rightarrow 0$ has little practical value. For very large $h^{-2} \delta t$, Proposition 2.4 suggests a *physics-based* (or more precisely, *PDE-based*) *nearest Kronecker product* (PNKP) preconditioner,

$$(2.4) \quad \mathcal{M}_{\text{PNKP}} = \delta t \mathbf{A} \otimes \mathbf{K}.$$

It is convenient to approximate the inverse of PNKP due to the inverse rule of the Kronecker product [22, Section 1.3.6],

$$(2.5) \quad (\mathbf{S} \otimes \mathbf{T})^{-1} = \mathbf{S}^{-1} \otimes \mathbf{T}^{-1}.$$

Hence, in PNKP, one only needs to (approximately) factorize \mathbf{K} . However, $\mathcal{M}_{\text{PNKP}}$ is expected to be effective only as $h^{-2} \delta t$ tends to ∞ . In the work, we will focus on moderately large time steps, i.e., $\delta t = \mathcal{O}(h^\alpha)$ for some $0 < \alpha \leq 1$. We will use $\mathcal{M}_{\text{PNKP}}$ as a baseline in comparison with other preconditioners in terms of efficiency and effectiveness for large $h^{-2} \delta t$.

2.3. State-of-the-Art Preconditioners for FIRK. We briefly review some existing preconditioners of FIRK, which were representative of state of the art prior to this work.

Block diagonal and block triangular preconditioners. One of the simplest and the most effective preconditioners for FIRK is the *block Gauss-Seidel (BGS)*, i.e.,

$$(2.6) \quad \mathcal{M}_{\text{BGS}} = \mathbf{I}_s \otimes \mathbf{M} + \delta t \mathbf{L} \otimes \mathbf{K},$$

where \mathbf{L} is the lower triangular part of \mathbf{A} . From Proposition 2.4, it is easy to see that BGS is mathematically optimal as $h^{-2}\delta t \rightarrow 0$, but not so as $h^{-2}\delta t \rightarrow \infty$. Hence, we expect BGS to perform well for small time steps but worse for large time steps. BGS was investigated by van der Houwen and de Swart in [48] along with other block-triangular preconditioners. They took advantage of the fact that the Butcher matrices from FIRK, such as those of Gauss-Legendre, Radau IIA, and Lobatto IIC, often have a dominant lower triangular part. Therefore, BGS performs significantly better than block diagonal [33] (BD, aka block Jacobi [37]) or block upper-triangular preconditioners. There were some attempts on improving BGS, such as [44], by replacing \mathbf{L} with a different lower-triangular matrix $\tilde{\mathbf{L}}$ that minimizes $\kappa(\mathbf{A}\tilde{\mathbf{L}}^{-1})$ under the constraint that $\text{diag}(\tilde{\mathbf{L}}) = \text{diag}(\mathbf{L})$. Our numerical results, however, show that the preconditioners in [44] often under-performed BGS. Hence, although simple, BGS is representative of the state-of-the-art block triangular preconditioner. \mathcal{M}_{BGS} has a similar cost per KSP iteration compared to PNKP. However, for the s -stage GL schemes, BGS needs to (approximately) factorize $\lceil s/2 \rceil$ distinct diagonal blocks because the diagonal of \mathbf{A} has $\lceil s/2 \rceil$ distinct values.

Block circulant preconditioners. Motivated by a Strang-type circulant preconditioner for Toeplitz-like matrices [4], Chan et al. [11] proposed a Strang-type block-circulant (BC) preconditioner for linear multistep formulas (LMF). Although high-order LMF is less desirable than implicit RK schemes due to their lack of A-stability [17], the idea of BC preconditioner can be adapted to FIRK [14, 49]. In this context, the preconditioner has the form

$$(2.7) \quad \mathcal{M}_{\text{BC}} = \mathbf{I}_s \otimes \mathbf{M} + \delta t \mathbf{C} \otimes \mathbf{K}$$

$$(2.8) \quad = (\mathbf{F} \otimes \mathbf{I}_n)(\mathbf{I}_s \otimes \mathbf{M} + \delta t \mathbf{\Lambda} \otimes \mathbf{K})(\mathbf{F}^H \otimes \mathbf{I}_n)$$

where $\mathbf{F} \in \mathbb{C}^{s \times s}$ is the normalized Fourier matrix (i.e., $\mathbf{F}\mathbf{F}^H = \mathbf{I}$), and $\mathbf{C} = \mathbf{F}\mathbf{\Lambda}\mathbf{F}^H$ is the Schur decomposition of a circulant matrix that approximates \mathbf{A} . From the inverse rule (2.5) and the product rule of the Kronecker product [22, Section 1.3.6],

$$(2.9) \quad (\mathbf{S} \otimes \mathbf{X})(\mathbf{T} \otimes \mathbf{Y}) = (\mathbf{ST}) \otimes (\mathbf{XY}),$$

we then obtain a closed-form expression

$$\mathcal{M}_{\text{BC}}^{-1} = (\mathbf{F} \otimes \mathbf{I}_n)(\mathbf{I}_s \otimes \mathbf{M} + \delta t \mathbf{\Lambda} \otimes \mathbf{K})^{-1}(\mathbf{F}^H \otimes \mathbf{I}_n),$$

where the matrix in the middle is block diagonal, of which the diagonal blocks need to be (approximately) factorized. The effectiveness of \mathcal{M}_{BC} depends on how well \mathbf{A} can be approximated by a circulant matrix. For Toeplitz-like matrices in MLF, \mathbf{C} can be constructed by minimizing $\|\mathbf{A} - \mathbf{C}\|_F$ [12]. More generally, \mathbf{C} can be constructed to minimize $\|\mathbf{I} - \mathbf{C}^{-1}\mathbf{A}\|_F$ [47]. It can be seen that \mathcal{M}_{BC} is optimal as $h^{-2}\delta t \rightarrow 0$. However, \mathcal{M}_{BC} requires complex arithmetic, and $\mathbf{\Lambda}$ in general has s distinct values. Hence, \mathcal{M}_{BC} is more expensive than BGS both in memory and computational cost per KSP iteration.

Kronecker product splitting preconditioners. More recently, H. Chen [13] proposed the so-called *Kronecker product splitting (KPS)* preconditioner, which has the form

$$(2.10) \quad \mathcal{M}_{\text{KPS}}(\alpha) = 1/2\alpha(\mathbf{I} + \alpha\mathbf{A}) \otimes (\delta t\mathbf{K} + \alpha\mathbf{M})$$

for some $\alpha > 0$, where $\delta t\mathbf{K} + \alpha\mathbf{M}$ needs to be (approximately) factorized. \mathcal{M}_{KPS} is a splitting preconditioner in that $\mathcal{A} = \mathcal{M}_{\text{KPS}}(\alpha) - 1/2\alpha(\mathbf{I} - \alpha\mathbf{A}) \otimes (\delta t\mathbf{K} - \alpha\mathbf{M})$. Chen chose α by minimizing $\max_{\mu \in \lambda(\mathbf{A}^{-1})} |(\mu - \alpha)/(\mu + \alpha)|$, where $\lambda(\mathbf{A}^{-1})$ denotes the eigenvalues of \mathbf{A}^{-1} . From Proposition 2.4, it is easy to show that \mathcal{M}_{KPS} is not optimal as $h^{-2}\delta t$ tends to 0, neither is it optimal as $h^{-2}\delta t$ tends to ∞ ; hence, we expect KPS to under-perform BGS and PNKP for small and large $h^{-2}\delta t$, respectively. In [14], H. Chen proposed a *generalized Kronecker product splitting (GKPS)* preconditioner

$$(2.11) \quad \mathcal{M}_{\text{GKPS}}(\alpha, \beta) = 1/(\alpha + \beta)(\mathbf{I} + \alpha\mathbf{A}) \otimes (\delta t\mathbf{K} + \beta\mathbf{M})$$

based on the splitting $\mathcal{A} = \mathcal{M}_{\text{GKPS}}(\alpha, \beta) - 1/(\alpha + \beta)(\mathbf{I} - \beta\mathbf{A}) \otimes (\delta t\mathbf{K} - \alpha\mathbf{M})$. The optimal choice of α and β requires the knowledge of the spectrum of $\mathbf{M}^{-1}\mathbf{K}$ [14]. Both KPS and GKPS can be interpreted as *NKP (near Kronecker product* [22, Section 12.3.7]) approximations of \mathbf{A} , and they are cheaper than BGS in terms of factorization cost and memory requirement. In terms of the number of GMRES iterations, KPS had mixed performance compared to BGS [13], so did GKPS [14]. Since it is difficult to optimize the parameters in GKPS, we will consider KPS instead of GKPS when comparing with our methods.

2.4. Single-level and multilevel incomplete factorization. The preconditioners mentioned above require (approximately) factorizing the diagonal blocks. *Incomplete LU (ILU)* is arguably the most promising for this purpose. Given a linear system $\mathcal{A}\mathcal{X} = \mathcal{B}$, ILU approximately factorizes \mathcal{A} by

$$(2.12) \quad \mathcal{P}^T \mathcal{A} \mathcal{Q} \approx \mathcal{L} \mathcal{D} \mathcal{U},$$

where \mathcal{D} is a diagonal matrix, and \mathcal{L} and \mathcal{U} are unit lower and upper triangular matrices, respectively. The permutation matrices \mathcal{P} and \mathcal{Q} may be constructed statically (such as using equilibration [19] or reordering [2]) and dynamically (such as by pivoting [38, 41]). We refer to (2.12) as *single-level ILU*. The simplest form of single-level ILU is ILU(0), which does not have any dynamic pivoting and preserves the sparsity patterns of the lower and upper triangular parts of $\mathcal{P}^T \mathcal{A} \mathcal{Q}$ in \mathcal{L} and \mathcal{U} , respectively. ILU(0) has linear time complexity in the number of nonzeros, and it is often effective for fluid problems [29, 36, 37]. For more challenging problems, ILU with dual thresholding (ILUT) [40] introduces *fills* based on the levels in the elimination tree and numerical values. One may also enable dynamic pivoting, leading to so-called ILUP [38] and ILUTP [41]. However, these more sophisticated variants often have superlinear time complexity [21], and they may suffer from small pivots or unstable triangular factors [42].

Multilevel incomplete LU (MLILU) is a general algebraic framework for building block preconditioners. More precisely, a two-level ILU reads

$$(2.13) \quad \mathcal{P}^T \mathcal{A} \mathcal{Q} = \begin{bmatrix} \mathbf{B} & \mathbf{F} \\ \mathbf{E} & \mathbf{C} \end{bmatrix} \approx \mathcal{M} = \begin{bmatrix} \tilde{\mathbf{B}} & \tilde{\mathbf{F}} \\ \tilde{\mathbf{E}} & \mathbf{C} \end{bmatrix} = \begin{bmatrix} \mathbf{L} & \mathbf{0} \\ \mathbf{L}_E & \mathbf{I} \end{bmatrix} \begin{bmatrix} \mathbf{D} & \mathbf{0} \\ \mathbf{0} & \mathbf{S}_C \end{bmatrix} \begin{bmatrix} \mathbf{U} & \mathbf{U}_F \\ \mathbf{0} & \mathbf{I} \end{bmatrix},$$

where $\mathbf{B} \approx \tilde{\mathbf{B}} = \mathbf{L} \mathbf{D} \mathbf{U}$ corresponds to a single-level ILU of the leading block, and $\mathbf{S}_C = \mathbf{C} - \mathbf{L}_E \mathbf{D} \mathbf{U}_F$ is the Schur complement. One can also apply dynamic pivoting [34] or deferring [7] in MLILU. For this two-level ILU, $\mathcal{P} \mathcal{M} \mathcal{Q}^T$ provides a preconditioner of \mathcal{A} . By factorizing \mathbf{S}_C in (2.13) recursively, we obtain an MLILU and a corresponding multilevel

preconditioner. The recursion terminates when the Schur complement is sufficiently small, and then a complete LU factorization can be employed. Compared to single-level ILU factorizations, MLILU is generally more robust and effective, especially for indefinite systems [15, 21].

In this work, we utilize a near-linear-complexity multilevel ILU called HILUCSI, which stands for *Hierarchical ILU-Crout with Scalability-oriented and Inverse-based dropping* [15]. HILUCSI shares some similarities with other MLILU (such as ILUPACK [6]). However, its *scalability-oriented dropping* enables near-linear time complexity in its factorization and triangular solves in the number of unknowns. We refer readers to [15] for details. The original implementation of HILUCSI in [15] only supported real arithmetic. We extended HILUCSI for this work to support complex arithmetic.

It is worth noting that one may attempt to apply a single-level or multilevel ILU to the coefficient matrix \mathcal{A} in (1.3) directly. However, the effectiveness of ILU decreases as the size of the matrices increases due to increased droppings. In addition, it is computationally expensive to apply multilevel ILU to \mathcal{A} directly for many-stage FIRK. Therefore, it is desirable to take advantage of the Kronecker-product structures, as we will demonstrate in Section 5.1.

3. Mathematically Optimal Preconditioners. We now introduce two optimal preconditioners based on the Schur decomposition and an alternative based on the Jordan form.

3.1. Block complex Schur decomposition. When $\delta t = \mathcal{O}(h^\alpha)$ for $\alpha \approx 1$, we must consider both Kronecker products in (1.3). To this end, we could consider a generalization of the block-circulant preconditioners. In particular, it is well known that there is a complex Schur decomposition (CSD) $\mathbf{A} = \mathbf{U}\mathbf{T}\mathbf{U}^H$ for any $\mathbf{A} \in \mathbb{C}^{s \times s}$, where $\mathbf{U} \in \mathbb{C}^{s \times s}$ is unitary and $\mathbf{T} \in \mathbb{C}^{s \times s}$ is upper triangular. Hence, we define a *block CSD (BCSD)* preconditioner analogous to \mathcal{M}_{BC} , namely,

$$\mathcal{M}_{\text{BCSD}} = (\mathbf{U} \otimes \mathbf{I}_n) \mathcal{T} (\mathbf{U}^H \otimes \mathbf{I}_n) \quad \text{with} \quad \mathcal{T} = \mathbf{I}_s \otimes \mathbf{M} + \delta t \mathbf{T} \otimes \mathbf{K},$$

where \mathcal{T} is block upper-triangular with $\mathbb{C}^{m \times m}$ diagonal blocks.

PROPOSITION 3.1. *BCSD preconditioner is mathematically optimal for \mathcal{A} .*

Proof. Using the product rule (2.9), $\mathcal{M}_{\text{BCSD}} = \mathcal{A}$ with exact factorization. \square

Remark 3.2. $\mathcal{M}_{\text{BCSD}}$ was motivated by \mathcal{M}_{BC} in (2.7) and it overcomes the approximation errors in the latter. \mathcal{M}_{BC} was originally designed for LMF, for which the matrix \mathbf{I}_s in (1.3) must be replaced by a general matrix \mathbf{B} . Note that $\mathcal{M}_{\text{BCSD}}$ can be generalized to LMF by using a generalized CSD [22, Section 7.7.2] on \mathbf{A} and \mathbf{B} .

In practice, we need to factorize the diagonal blocks in \mathcal{T} approximately. In this case, $\mathcal{M}_{\text{BCSD}}$ is ϵ -accurate with a sufficiently accurate approximate factorization.

THEOREM 3.3. *Given $\tilde{\mathcal{T}} = \mathcal{T} + \delta \mathcal{T}$ such that $\|\tilde{\mathcal{T}}^{-1}\| \leq C$ for some bounded $C > 0$, $\tilde{\mathcal{M}} = (\mathbf{U} \otimes \mathbf{I}_n) \tilde{\mathcal{T}} (\mathbf{U}^H \otimes \mathbf{I}_n)$ is an ϵ -accurate preconditioner with sufficiently small $\|\delta \mathcal{T}\|$.*

Proof. Let $\mathcal{X} = \mathbf{U} \otimes \mathbf{I}_n$ in Definition 2.1. Then, $\mathcal{X}^{-1} = \mathbf{U}^H \otimes \mathbf{I}_n$ and

$$\begin{aligned} \left\| \mathcal{X}^{-1} \left(\mathcal{A} \tilde{\mathcal{M}}^{-1} \right) \mathcal{X} - \mathbf{I} \right\| &= \left\| \mathcal{X}^{-1} \left(\mathcal{M}_{\text{BCSD}} \tilde{\mathcal{M}}^{-1} \right) \mathcal{X} - \mathbf{I} \right\| \\ &= \left\| \mathcal{T} \tilde{\mathcal{T}}^{-1} - \mathbf{I} \right\| \\ &= \left\| \delta \mathcal{T} \tilde{\mathcal{T}}^{-1} \right\|, \end{aligned}$$

which is bounded by $\|\delta \mathcal{T}\| C$. Hence, $\tilde{\mathcal{M}}$ is ϵ -accurate with a bounded C and sufficiently small $\|\delta \mathcal{T}\|$. \square

When using HILUCSI to factorize its diagonal blocks, the boundedness of $\|\tilde{\mathcal{T}}^{-1}\|$ is ensured, since HILUCSI monitors and dynamically controls the condition numbers of the triangular and diagonal factors using permutations. For sufficiently tight dropping thresholds in HILUCSI, $\|\delta\mathcal{T}\| \ll 1/\|\tilde{\mathcal{T}}^{-1}\|$. In addition, $\|\delta\mathcal{T}\|$ tends to be smaller for small $h^{-2}\delta t$ due to the (block) diagonal dominance of $\mathbf{I}_s \otimes \mathbf{M}$.

3.2. Ordering of BCSD. CSD is not unique, and any ordering of the eigenvalues in its diagonal entries suffices in exact arithmetic. With incomplete factorization of the diagonal blocks, different decompositions may lead to different convergence rates of GMRES. To optimize the ordering, we derive an error analysis for BCSD as follows.

LEMMA 3.4. *Suppose that the diagonal blocks $\mathbf{D}_i \in \mathbb{C}^{m \times m}$ of $\mathcal{T} \in \mathbb{C}^{sm \times sm}$ are approximated by $\tilde{\mathbf{D}}_i = \mathbf{D}_i + \delta\mathbf{D}_i$, while the off-diagonal blocks \mathbf{T}_{ij} are exact. Let $\delta\mathcal{D}$ be the block diagonal matrix composed of $\delta\mathbf{D}_i$, $\tilde{\mathcal{T}} = \mathcal{T} + \delta\mathcal{D}$, and $\tilde{\mathcal{M}} = (\mathbf{U} \otimes \mathbf{I}_m)\tilde{\mathcal{T}}(\mathbf{U}^H \otimes \mathbf{I}_m)$. Given a vector $\mathcal{B} \in \mathbb{C}^m$, let $\mathcal{Y} = (\mathbf{U}^H \otimes \mathbf{I}_m)\mathcal{M}_{\text{BCSD}}^{-1}\mathcal{B}$ and $\tilde{\mathcal{Y}} = \mathcal{Y} + \delta\mathcal{Y} = (\mathbf{U}^H \otimes \mathbf{I}_m)\tilde{\mathcal{M}}^{-1}\mathcal{B}$. Then,*

$$(3.1) \quad \mathcal{T}\delta\mathcal{Y} = -\delta\mathcal{D}\tilde{\mathcal{Y}}.$$

For convenience, let \mathbf{y}_i , $\tilde{\mathbf{y}}_i$ and $\delta\mathbf{y}_i$ denote the i th block in \mathcal{Y} , $\tilde{\mathcal{Y}}$, and $\delta\mathcal{Y}$ corresponding to \mathbf{D}_i , respectively.

Proof. Let $\hat{\mathbf{b}}_i$ denote the i th block in $(\mathbf{U}^H \otimes \mathbf{I}_m)\mathcal{B}$. By definition,

$$\tilde{\mathbf{D}}_i\tilde{\mathbf{y}}_i + \sum_{j=i+1}^s \mathbf{T}_{ij}\tilde{\mathbf{y}}_j = \hat{\mathbf{b}}_i = \mathbf{D}_i\mathbf{y}_i + \sum_{j=i+1}^s \mathbf{T}_{ij}\mathbf{y}_j.$$

Hence, $\mathbf{D}_i\delta\mathbf{y}_i + \sum_{j=i+1}^s \mathbf{T}_{ij}\delta\mathbf{y}_j = -\delta\mathbf{D}_i\tilde{\mathbf{y}}_i$, and equivalently (3.1). \square

Note that $\|\mathcal{T}^{-1}\|$ is invariant of the ordering. From a standard norm-wise error analysis $\|\delta\mathcal{Y}\| \leq \|\mathcal{T}^{-1}\| \|\delta\mathcal{D}\tilde{\mathcal{Y}}\|$, one may conclude that $\|\delta\mathcal{Y}\|$ is insensitive to the ordering, assuming $\|\tilde{\mathcal{Y}}\| \approx \|\mathcal{Y}\|$. However, the following asymptotic analysis suggests that the component-wise errors do depend on the ordering of CSD and may be optimized under some reasonable assumptions.

PROPOSITION 3.5. *Assume $\|\delta\mathcal{D}\| = \mathcal{O}(\varepsilon)$ for some small ε and $\|\mathbf{D}_i^{-1}\| = \mathcal{O}(1)$. Then,*

$$(3.2) \quad \|\delta\mathbf{y}_i\| \leq \|\mathbf{D}_i^{-1}\| \left(\|\delta\mathbf{D}_i\mathbf{y}_i\| + \sum_{j=i+1}^s \|\mathbf{T}_{ij}\| \|\delta\mathbf{y}_j\| \right) + \mathcal{O}(\varepsilon^2).$$

Proof. Due to Lemma 3.4,

$$(3.3) \quad \mathbf{D}_i\delta\mathbf{y}_i = - \sum_{j=i+1}^s \mathbf{T}_{ij}\delta\mathbf{y}_j - \delta\mathbf{D}_i\tilde{\mathbf{y}}_i = - \sum_{j=i+1}^s \mathbf{T}_{ij}\delta\mathbf{y}_j - \delta\mathbf{D}_i\mathbf{y}_i - \delta\mathbf{D}_i\delta\mathbf{y}_i.$$

Expanding the recursion, we conclude that $\|\delta\mathbf{y}_i\| = \mathcal{O}(\|\delta\mathcal{D}\|) = \mathcal{O}(\varepsilon)$ for a constant s . Hence, $\|\delta\mathbf{D}_i\delta\mathbf{y}_i\| \leq \|\delta\mathbf{D}_i\| \|\delta\mathbf{y}_i\| = \mathcal{O}(\varepsilon^2)$, and (3.2) then follows from (3.3). \square

Let d_i denote the i th diagonal block in \mathbf{T} in CSD. Note that as $h^{-2}\delta t$ tends to ∞ , $\|\mathbf{D}_i^{-1}\|$ tends to $|d_i^{-1}| \|\mathbf{K}^{-1}\|$. For FDM, $\|\mathbf{K}^{-1}\| = \mathcal{O}(1)$ (due to a similar argument as Lemma 2.3), so the assumption of $\|\mathbf{D}_i^{-1}\| = \mathcal{O}(1)$ is reasonable; for FEM, $\|\mathbf{K}^{-1}\| = \mathcal{O}(1) \|\mathbf{M}^{-1}\|$ [20], so we need to generalize the assumptions to take into account $\|\mathbf{M}^{-1}\|$. In either case, following a similar procedure as in the backward error analysis for back solve [46, pp. 122–127], we can conclude that the recursions in (3.2) would lead to an amplification factor of

$\prod_{k=j}^s \|D_k^{-1}\| \|T_{jk}\|$ on $\|\delta D_j \mathbf{y}_j\|$ for $i+1 \leq j \leq s$ in $\|\delta \mathbf{y}_i\|$. Assuming $|d_i^{-1}| > 1$ and $\|\delta D_j \mathbf{y}_j\|$ and $\|T_{ij}\|$ are insensitive to reordering, we can decrease these amplification factors by making $|d_i^{-1}| = 1/|d_i|$ as small as possible for large i in T . Hence, we order the CSD so that $|d_i|$ is in ascending order. We will demonstrate the benefit of this ordering for the five- and six-stage GL schemes in Section 5.3. To compute this ordering, one can use the MATLAB code in [8] to sort the real Schur decomposition (RSD) based on the complex eigenvalues, and then convert the RSD to CSD using the MATLAB function `rsf2csf` [45].

3.3. Block real Schur decomposition. For IRK, $A \in \mathbb{R}^{s \times s}$, and there is a *real Schur decomposition (RSD)* [22, Section 7.4.1],

$$(3.4) \quad A = QRQ^T,$$

where $Q \in \mathbb{R}^{s \times s}$ is orthogonal (i.e., $QQ^T = I$) and $R \in \mathbb{R}^{s \times s}$ is *quasi-triangular*, with 1-by-1 and 2-by-2 diagonal blocks. We define a *block RSD (BRSD)* preconditioner as

$$(3.5) \quad \mathcal{M}_{\text{BRSD}} = (Q \otimes I_n) \mathcal{R} (Q^T \otimes I_n) \quad \text{with} \quad \mathcal{R} = I_s \otimes M + \delta t R \otimes K,$$

where \mathcal{R} is block quasi-triangular with $\mathbb{R}^{m \times m}$ and $\mathbb{R}^{2m \times 2m}$ diagonal blocks.

PROPOSITION 3.6. *BRSD preconditioner is mathematically optimal for \mathcal{A} .*

Proof. It follows from the same argument as Proposition 3.1. \square

Like $\mathcal{M}_{\text{BCSD}}$, $\mathcal{M}_{\text{BRSD}}$ can also be generalized to LMF by using a generalized RSD [22, Section 7.7.2]. BRSD requires only real arithmetic. However, its larger $2m \times 2m$ blocks are more expensive to factorize than the $m \times m$ complex-valued blocks in BCSD. In addition, the larger blocks in BRSD may also decrease its effectiveness compared to BCSD, as we will demonstrate in Section 5.2.

Like CSD, RSD is not unique, and different ordering may lead to different convergence rate. We can generalize the analysis in Proposition 3.5 and then assume $\|\delta D_j \mathbf{x}_j\|$ and $\|R_{ij}\|$ are insensitive to the ordering for the diagonal blocks $D_i \in \mathbb{R}^{2m \times 2m} \cup \mathbb{R}^{m \times m}$ and off-diagonal blocks $R_{ij} \in \mathbb{R}^{2m \times 2m} \cup \mathbb{R}^{m \times m}$ of $\mathcal{R} \in \mathbb{R}^{sm \times sm}$. Such an assumption seems reasonable for even-stage GL. For odd-stage GL, we put the 1-by-1 diagonal block corresponding to the real eigenvalue at the upper-left corner of R in (3.4), and then a similar assumption seems reasonable to the other blocks. Our numerical experiments show that such an ordering indeed improves the effectiveness of BRSD for GL schemes. In addition, we observed that this ordering for GL schemes coincides with sorting the real parts of the eigenvalues of RSD in descending order. For completeness, we describe the procedure in Appendix A. As examples, Table 3.1 shows the Q and R matrices of BRSD for the three- and four-stage GL schemes; for the two-stage GL, $Q = I_2$ and $R = A$.

3.4. Block Jordan form. As an alternative to BCSD and BRSD, one might utilize a Jordan decomposition $A = X \Lambda X^{-1}$ to construct a *block Jordan form (BJF)* preconditioner

$$(3.6) \quad \mathcal{M}_{\text{BJF}} = (X \otimes I_n) (I_s \otimes M + \delta t \Lambda \otimes K) (X^{-1} \otimes I_n),$$

where X and Λ are in $\mathbb{C}^{s \times s}$. If A is nondefective, as in GL schemes, then Λ is diagonal and contains (complex) eigenvalues. This block Jordan form was developed as a solution technique for IRK independently by Butcher [9] and Bickart [5]; see also [23, p. 122]. It was also leveraged recently in [24] in analyzing the condition numbers of IRK in conjunction with diagonal preconditioners. To the best of our knowledge, BJF has not been used as a preconditioner for IRK in the literature. Hence, we consider it as a new preconditioning technique motivated by Butcher [9] and Bickart [5]. Like BCSD, BJF also requires complex

Table 3.1: The \mathbf{Q} and \mathbf{R} matrices for BRSD from a sorted and permuted real Schur forms of the Butcher matrices for the three and four-stage GL schemes.

s	BRSD (\mathbf{Q})	BRSD (\mathbf{R})
3	$\begin{bmatrix} 0.0715 & -0.1246 & -0.9896 \\ 0.1177 & 0.9863 & -0.1157 \\ 0.9905 & -0.1082 & 0.0852 \end{bmatrix}$	$\begin{bmatrix} 0.2153 & 0.4392 & -0.3537 \\ 0 & 0.1423 & -0.2704 \\ 0 & 0.0682 & 0.1423 \end{bmatrix}$
4	$\begin{bmatrix} -0.0117 & 0.2096 & 0.3219 & 0.9232 \\ 0.0283 & 0.1012 & -0.9458 & 0.3072 \\ 0.1826 & 0.9561 & 0.0342 & -0.2267 \\ 0.9827 & -0.1780 & 0.0247 & 0.0442 \end{bmatrix}$	$\begin{bmatrix} 0.1584 & 0.4262 & -0.2749 & 0.2277 \\ -0.0053 & 0.1584 & -0.2219 & 0.2206 \\ 0 & 0 & 0.0916 & -0.1834 \\ 0 & 0 & 0.0729 & 0.0916 \end{bmatrix}$

arithmetic, and it is mathematically optimal in exact arithmetic. However, BJB cannot be generalized to LMF. More importantly, BJB is not ϵ -accurate with incomplete factorization for GL-schemes with large s , because \mathbf{X} in (3.6) is not orthogonal in general and there is empirical evidence that $\kappa(\mathbf{X})$ grows nearly exponentially in s . Nevertheless, it is worth considering BJB for small s .

4. Near-Optimal Preconditioners. We now introduce a ‘‘singly diagonal’’ approximation of BRSD with reduced cost. We also compare it qualitatively with others.

4.1. Singly-diagonal approximate BRSD. We now describe a *singly-diagonal approximate BRSD* (SABRSD) preconditioner,

$$(4.1) \quad \mathcal{M}_{\text{SABRSD}} = (\mathbf{Q} \otimes \mathbf{I}_n) \hat{\mathcal{R}} (\mathbf{Q}^T \otimes \mathbf{I}_n), \text{ where } \hat{\mathcal{R}} = \mathbf{I}_s \otimes \mathbf{M} + \delta t \hat{\mathbf{R}} \otimes \mathbf{K},$$

where $\hat{\mathbf{R}}$ is a *singly diagonally upper triangular* (SDUT) matrix, i.e., a scalar multiple of a unit upper triangular matrix. Let \mathbb{T}_s denote the set of $s \times s$ SDUT matrices, i.e., $\mathbb{T}_s = \{\mathbf{T} \in \mathbb{R}^{s \times s} \mid t_{ii} = t_{jj} \wedge t_{ij} = 0, \forall j < i\}$. We compute $\hat{\mathbf{R}}$ to approximate \mathbf{R} in (3.4) using a constrained minimization

$$(4.2) \quad \hat{\mathbf{R}} = \arg \min_{\hat{\mathbf{R}} \in \mathbb{T}_s} \left\| \mathbf{I} - \mathbf{R} \hat{\mathbf{R}}^{-1} \right\| \quad \text{subject to} \quad \min_{\hat{\mathbf{R}} \in \mathbb{T}_s} \kappa(\mathbf{R} \hat{\mathbf{R}}^{-1}).$$

Remark 4.1. The objective function in (4.2) shares some similarity with that in [47] for the ‘‘superoptimal’’ condition for a circulant left-preconditioner \mathbf{C} , where Tyrtshnikov minimized $\|\mathbf{I} - \mathbf{C}^{-1} \mathbf{A}\|_F$ without an analogous constraint on $\kappa(\mathbf{C}^{-1} \mathbf{A})$. Our constraint on $\kappa(\mathbf{R} \hat{\mathbf{R}}^{-1})$ is similar to the objective function used by Staff et al. [44] in optimizing a block lower-triangular preconditioner (analogous to $\hat{\mathbf{R}}^T$ if we replace \mathbf{Q} with \mathbf{I}_s), where they set the diagonal entries of $\hat{\mathbf{R}}^T$ to be those in \mathbf{A} without taking into account $\|\mathbf{I} - \mathbf{R} \hat{\mathbf{R}}^{-1}\|$.

The dual conditions in (4.2) were motivated our numerical experimentation; see Section 5.4. We can also derive them based on Definition 2.1. Let us assume $\delta t \gtrsim \mathcal{O}(h)$, so $h^{-2} \delta t \gg 1$. In this case, \mathbf{K} dominates \mathbf{M} , so it is reasonable to absorb the perturbations due to the approximate factorization into \mathbf{K} , so that $\mathbf{I}_s \otimes \mathbf{M} + \delta t \mathbf{R} \otimes \mathbf{K}$ is approximated by $\mathbf{I}_s \otimes \mathbf{M} + \delta t \hat{\mathbf{R}} \otimes \hat{\mathbf{K}}$, where $\hat{\mathbf{R}} = \mathbf{R} + \delta \mathbf{R}$ and $\hat{\mathbf{K}} = \mathbf{K} + \delta \mathbf{K}$. Hence,

$\mathbf{I}_s \otimes \mathbf{M} + \delta t \mathbf{R} \otimes \mathbf{K} \approx \delta t \hat{\mathbf{R}} \otimes \tilde{\mathbf{K}}$ and $\mathbf{I}_s \otimes \mathbf{M} + \delta t \hat{\mathbf{R}} \otimes \tilde{\mathbf{K}} \approx \delta t \hat{\mathbf{R}} \otimes \tilde{\mathbf{K}}$. Then,

$$\begin{aligned} & \|(\mathbf{Q} \otimes \mathbf{I})(\mathbf{I}_s \otimes \mathbf{M} + \delta t \mathbf{R} \otimes \mathbf{K})(\mathbf{I}_s \otimes \mathbf{M} + \delta t \hat{\mathbf{R}} \otimes \tilde{\mathbf{K}})^{-1}(\mathbf{Q}^T \otimes \mathbf{I}) - \mathbf{I}\| \\ & \approx \|(\mathbf{R} \otimes \mathbf{K})(\hat{\mathbf{R}} \otimes \tilde{\mathbf{K}})^{-1} - \mathbf{I}\| \\ & = \left\| \left((\hat{\mathbf{R}} - \delta \mathbf{R}) \hat{\mathbf{R}}^{-1} \right) \otimes \left((\tilde{\mathbf{K}} - \delta \mathbf{K}) \tilde{\mathbf{K}}^{-1} \right) - \mathbf{I} \right\| \\ & = \left\| \delta \mathbf{R} \hat{\mathbf{R}}^{-1} \otimes \mathbf{I}_m + \mathbf{R} \hat{\mathbf{R}}^{-1} \otimes (\delta \mathbf{K} \tilde{\mathbf{K}}^{-1}) \right\| \\ & \leq \left\| \mathbf{I} - \mathbf{R} \hat{\mathbf{R}}^{-1} \right\| + \left\| \mathbf{R} \hat{\mathbf{R}}^{-1} \right\| \otimes \left\| \delta \mathbf{K} \tilde{\mathbf{K}}^{-1} \right\|. \end{aligned}$$

In (4.2), the constraint $\min \kappa(\mathbf{R} \hat{\mathbf{R}}^{-1})$, where $\kappa(\mathbf{R} \hat{\mathbf{R}}^{-1}) = \left\| \hat{\mathbf{R}} \mathbf{R}^{-1} \right\| \left\| \mathbf{R} \hat{\mathbf{R}}^{-1} \right\|$ ensures a bounded $\left\| \mathbf{R} \hat{\mathbf{R}}^{-1} \right\|$, assuming $\left\| \hat{\mathbf{R}} \mathbf{R}^{-1} \right\|$ is nearly a constant. Note that $\kappa(\mathbf{R} \hat{\mathbf{R}}^{-1})$ is invariant under scaling of $\hat{\mathbf{R}}$. The minimization of $\left\| \mathbf{I} - \mathbf{R} \hat{\mathbf{R}}^{-1} \right\|$ determines the scaling factor of $\hat{\mathbf{R}}$. Due to its singly-diagonal property, SABRSD has comparable cost as PNKP, assuming the overhead in multiplying vectors with \mathbf{Q} and \mathbf{Q}^T is negligible.

4.2. Ordering and permuting RSD for SABRSD. Similar to BRSD, the ordering of the eigenvalues along the diagonal blocks in RSD can affect the effectiveness of SABRSD. To derive an optimal order, assume the lower-triangular part of \mathbf{R} is negligible. In this case, Proposition 3.5 suggests that it is desirable to sort the diagonal entries in \mathbf{R} in ascending order, in contrast to descending order in $\mathcal{M}_{\text{BRSD}}$. To make the lower-triangular part negligible, we make the 2-by-2 diagonal blocks in \mathbf{R} as upper-triangularly dominant as possible, by making use of the following fact.

PROPOSITION 4.2. *Let $\mathbf{D} = \begin{bmatrix} \alpha & \gamma \\ \beta & \alpha \end{bmatrix}$ with $\alpha > 0$ and $\beta\gamma < 0$, and let \mathbf{S} be an orthogonal matrix. The lower-triangular component in $\tilde{\mathbf{D}} = \mathbf{S} \mathbf{D} \mathbf{S}^T$ attains the minimal magnitude when $\mathbf{S} = \mathbf{I}_2$ and $\mathbf{S} = \begin{bmatrix} 0 & 1 \\ 1 & 0 \end{bmatrix}$ for $|\beta| \leq |\gamma|$ and $|\beta| > |\gamma|$, respectively.*

Proof. Consider rotation $\mathbf{S}_\theta = \begin{bmatrix} \cos \theta & \sin \theta \\ -\sin \theta & \cos \theta \end{bmatrix}$, and then $\tilde{d}_{21} = \gamma - (\beta + \gamma) \sin(2\theta)$. $|\tilde{d}_{21}|$ is minimized when $\theta = 0$ and $\theta = \pi/2$ for $|\beta| \leq |\gamma|$ and $|\beta| > |\gamma|$, respectively. For $\theta = \pi/2$, $\mathbf{S} = \begin{bmatrix} 0 & 1 \\ 1 & 0 \end{bmatrix}$ flips the sign of the second row in \mathbf{S}_θ . \square

In Proposition 4.2, $\beta\gamma < 0$ is satisfied for any 2-by-2 diagonal block in RSD; the assumption of $\alpha > 0$ is equivalent to requiring the real parts for the eigenvalues of the Butcher matrix \mathbf{A} to be positive, which is valid for A-stable FIRK with an invertible \mathbf{A} [23, p. 402]. We will demonstrate the benefit of this ordering strategy in Section 5.3. Given the resulting RSD, $\hat{\mathbf{R}}$ in (4.1) can be obtained by using the optimization procedure described in Appendix B. Table 4.1 gives the \mathbf{Q} and $\hat{\mathbf{R}}$ matrices for the two-, three- and four-stage GL schemes.

4.3. Alternative approximations to BRSD. It is well known that the Butcher matrix \mathbf{A} is strongly lower-triangular dominant in GL schemes [48]. Hence, one may fix \mathbf{Q} in SABRSD to be the “flipped” identity matrix $\mathbf{P} = [\mathbf{e}_s, \mathbf{e}_{s-1}, \dots, \mathbf{e}_1]$, so that $\mathbf{P} \mathbf{A} \mathbf{P}^T$ is nearly upper triangular. Let $\hat{\mathbf{L}} = \mathbf{P} \hat{\mathbf{R}} \mathbf{P}$ minimize $\|\mathbf{I} - \mathbf{P} \mathbf{A} \mathbf{P}^T \hat{\mathbf{L}}^{-1}\| = \|\mathbf{I} - \mathbf{A} \hat{\mathbf{L}}^{-1}\|$ subject to the diagonal entries in $\hat{\mathbf{L}}$ being equal. This leads to a simple preconditioner

$$(4.3) \quad \mathcal{M}_{\text{SOBT}} = \mathbf{I}_s \otimes \mathbf{M} + \delta t \hat{\mathbf{L}} \otimes \mathbf{K},$$

Table 4.1: The Q and \hat{R} matrices of SABRSD for GL schemes with two to four stages.

s	SABRSD (Q)	SABRSD (\hat{R})
2	$\begin{bmatrix} 0 & 1 \\ 1 & 0 \end{bmatrix}$	$\begin{bmatrix} 0.3008 & 0.5876 \\ 0 & 0.3008 \end{bmatrix}$
3	$\begin{bmatrix} 0.0832 & -0.1811 & -0.9799 \\ -0.0603 & 0.9806 & -0.1863 \\ -0.9947 & -0.0746 & -0.0707 \end{bmatrix}$	$\begin{bmatrix} 0.2339 & -0.5739 & 0.4284 \\ 0 & 0.2339 & -0.3351 \\ 0 & 0 & 0.2339 \end{bmatrix}$
4	$\begin{bmatrix} -0.0482 & -0.0225 & 0.3367 & 0.9401 \\ 0.1222 & -0.0925 & -0.9290 & 0.3368 \\ -0.1117 & 0.9879 & -0.0943 & 0.0517 \\ -0.9850 & -0.1224 & -0.1211 & -0.0101 \end{bmatrix}$	$\begin{bmatrix} 0.212 & -0.535 & 0.3444 & -0.3663 \\ 0 & 0.212 & -0.3338 & 0.3178 \\ 0 & 0 & 0.212 & -0.274 \\ 0 & 0 & 0 & 0.212 \end{bmatrix}$

which we refer to as a *singly-diagonal optimized block triangular (SOBT)* preconditioner. SOBT is similar to the optimized block triangular preconditioners in Staff et al. [44], except that we use a different constrained minimization (4.2). One can compute SOBT by modifying the procedure described in Appendix B to minimize $\|I - \mathbf{A}\hat{L}^{-1}\|$. Compared to SABRSD, SOBT does not consider the ordering of the diagonal entries in the original matrix.

As another alternative approximation of BRSD, one may also simply use the upper-triangular part of BRSD as \hat{R} with the same ordering as SABRSD, instead of minimizing the objective function (4.2). We refer to this second alternative as *truncated BRSD* (or *TBRSD*). Compared to SABRSD, TBRSD does not minimize the errors based on ϵ -accuracy in Definition 2.1; it is also more expensive in that it requires factoring $\lceil s/2 \rceil$ diagonal blocks. In Section 5.4, we will compare SABRSD with SOBT and TBRSD to assess the effectiveness of our singly-diagonal optimization.

4.4. Qualitative comparison of preconditioners. We compare the advantages and disadvantages of some block preconditioners qualitatively, in terms of near-optimality, the number of real or complex factorizations, the number of real or complex solves of the diagonal blocks, and the available parallelism in concurrent solves of these diagonal blocks. Table 4.2 summarizes the comparison of nine block preconditioners, where the first five were reviewed in Section 2 and the others were introduced in this work. Among these preconditioners, BCSD, BRSD, and BJB are mathematically optimal block preconditioners for GL, assuming complete factorization and exact arithmetic. Among these three, BJB suffers from instability for large s . PNKP and SABRSD are near-optimal for large and intermediate time steps. In terms of factorization cost, we assume a two-way symmetry along its diagonal (i.e., $a_{i,i} = a_{s-i,s-i}$ for $i = 1, \dots, \lfloor s \rfloor$) for BD and BGS; we assume that there are $\lfloor s/2 \rfloor$ conjugate pairs of complex eigenvalues for BC, BJB, and BCSD, so that the factorization cost can be approximately halved by taking advantage of the fact that $\overline{M^{-1}\mathbf{b}} = \overline{M}^{-1}\overline{\mathbf{b}}$. Both of these properties can be verified for GL schemes. Under these assumptions, assuming near-linear scaling of the approximate factorization, BRSD requires about twice as much memory and factorization time as BD and BGS; the costs of BC, BJB, and BCSD are comparable to BRSD. SABRSD has the lowest memory requirement and factorization cost, comparable to PNKP and (G)KPS. In terms of the solve time, SABRSD is comparable with BGS, PNKP, and (G)KPS; BRSD is about twice as expensive; BCSD requires two to four times floating-point operations due to complex arithmetic, and similarly for BC and BJB. In terms of parallelism, BD, (G)KPS, BC, BJB, and PNKP enjoy s independent solves on the diagonal blocks. In

Table 4.2: Comparison of preconditioners for s -stage GL schemes. Last four are introduced in this section. “Parallel” indicates s independent solves on the diagonal blocks of \mathcal{A} .

preconditioner	near-optimal	factorization	solves	parallel
block diagonal [36]	$h^{-2}\delta t \rightarrow 0$	$\lceil s/2 \rceil \times \mathbb{R}^{m \times m}$	$s \times \mathbb{R}^{m \times m}$	✓
block Gauss-Seidel [48]				—
(G)KPS [13, 14]	—	$1 \times \mathbb{R}^{m \times m}$	$s \times \mathbb{R}^{m \times m}$	✓
block circulant [11, 49]	—	$\lceil s/2 \rceil \times \mathbb{C}^{m \times m}$ & $(s \bmod 2) \times \mathbb{R}^{m \times m}$	$s \times \mathbb{C}^{m \times m}$	✓
block Jordan form [24]	small s			✓
block CSD (BCSD)	optimal			—
block RSD (BRSD)	optimal	$\lceil s/2 \rceil \times \mathbb{R}^{2m \times 2m}$ & $(s \bmod 2) \times \mathbb{R}^{m \times m}$		—
PNKP	$h^{-2}\delta t \rightarrow \infty$	$1 \times \mathbb{R}^{m \times m}$	$s \times \mathbb{R}^{m \times m}$	✓
SABRS	$\delta t \gtrsim \mathcal{O}(h)$			—

contrast, the others require a block back solve, for which the s solves need to be performed in a serial order.

For BCSD, BRSD, PNKP, and SABRS, the conclusions in Table 4.2 hold for other FIRK schemes, assuming their Butcher matrices have $\lceil s/2 \rceil$ distinct complex conjugate pairs of eigenvalues. However, some conclusions for other preconditioners may change. In particular, the two-way symmetry of the diagonal entries does not hold for Radau and some other FIRK schemes, so the number of factorizations for BD and BGS would be s instead of $\lceil s/2 \rceil$.

5. Numerical Experimentation. In this section, we report numerical experimentation with the preconditioners introduced in Sections 3 and 4, and compare them with some others that we reviewed in Section 2.3. We discretized the 3D AD equation (1.1) using both FEM and FDM on $\Omega = [0, 1]^3$ with $\mu = 1$ and velocities $\mathbf{v} = [10, 10, 10]^T$ and $\mathbf{v} = [1, 1, 1]^T$, respectively. We conducted our numerical experiments using the method of *manufactured solutions*. Specifically, we used the following manufactured solution

$$(5.1) \quad u(x, y, z, t) = \sin(1.5\pi t) \sin(\pi x) \sin(\pi y) \sin(\pi z),$$

which generalized the 2D test case in [13, Section 5.2]. This manufactured solution has homogeneous boundary conditions at all time steps. For FEM, we used FEniCS 2019.1.0 [1, 32] to assemble the mass matrix M and the stiffness matrix K in (2.2) using a series of tetrahedral meshes with quadratic, cubic, and quartic (i.e., P_2 , P_3 , and P_4 , correspondingly) Lagrange elements. Table 5.1 shows the degrees of freedom (DOF) and the numbers of nonzeros (NNZ) in M and K for each testing case. For FDM, we used our in-house MATLAB code to construct the stiffness matrix K in (2.3) on a series of equidistant structured meshes with $h = 1/32$, $1/64$, and $1/128$, where one-sided stencils are used near the boundary. Table 5.2 shows the DOFs and NNZ in K for FDM testing cases. We discretized the resulting systems of ODEs using the GL schemes. For an s -stage GL scheme, the DOFs of \mathcal{A} in (1.3) are s times of those in Tables 5.1 and 5.2. For example, for the five-stage GL scheme on the finest mesh, there are more than ten million DOFs in \mathcal{A} for both FEM and FDM.

In all of our tests, we solved systems $\mathcal{A}\mathcal{U} = \mathcal{B}$ using our in-house MATLAB implementation of right-preconditioned restarted GMRES based on [39]. We limited the dimension of the Krylov subspace to 30 (i.e., GMRES(30)) and limited the maximum number of iterations to 500. For the convergence criterion, we used different relative tolerance (aka *rtol* or ε), i.e.,

Table 5.1: Statistics of testing cases using 3D FEM discretization. DOF and NNZ stand for degrees of freedom and number of nonzeros in \mathbf{K}_{FEM} in (2.2), respectively.

elem.	$\ell = 1$		$\ell = 2$		$\ell = 3$	
	DOF	NNZ	DOF	NNZ	DOF	NNZ
P_2	3,375	79,183	29,791	776,879	250,047	6,853,231
P_3	12,167	497,723	103,823	4,637,699	857,375	39,951,635
P_4	29,791	1,936,927	250,047	17,530,591	2,048,383	148,960,351

Table 5.2: Statistics of testing cases using 3D FDM discretization. DOF and NNZ stand for degrees of freedom and number of nonzeros in \mathbf{K}_{FDM} in (2.3), respectively.

stencil	$h = 1/32$		$h = 1/64$		$h = 1/128$	
	DOF	NNZ	DOF	NNZ	DOF	NNZ
$p = 2$		202,771		1,726,515		14,241,907
$p = 4$	29,791	381,517	250,047	3,226,797	2,048,383	26,532,205
$p = 6$		560,263		4,727,079		38,822,503

$\|\mathcal{B} - \mathcal{AU}\| \leq \varepsilon \|\mathcal{B}\|$. In terms of the initial guess of GMRES, we used the initial condition for the first time step and used the solution from the previous time step starting from second iterations. To get a reliable count on the numbers of iterations, we ran each test case for ten time steps and averaged the iteration counts starting from the second iteration.

5.1. Comparison of near-linear approximate inverses. The near-optimality requires near-linear complexity of approximate inverses in terms of both factorization and solve times per KSP iteration. As discussed in Section 2.4, ILU(0) and HILUCSI are two techniques that satisfy this requirement. To choose a proper one for our more detailed comparisons, we first compare these techniques as “global” preconditioners (i.e., approximately factorizing the $sm \times sm$ coefficient matrix \mathcal{A} directly) or for factorizing the diagonal blocks in BJB, KPS, and BGS. Although BJB was not previously used as a preconditioner in the literature, it shares some similarities with the Strang-type block-circulant preconditioners [11], so we include it in this baseline comparison.

Table 5.3 compares the average number of GMRES iterations as well as the average solve times per time step for the three-stage GL (GL-3) scheme with P_3 FEM on the two coarser meshes. In terms of the solve times, we include only the (block) triangular solves and the sparse matrix-vector multiplication, since they are the most dominant parts. All of timing was conducted on a single node of a Linux cluster with dual 2.60 GHz Intel(R) Xeon(R) E5-2690v3 processors with 128 GB RAM. HILUCSI is written in C++ [15], and we compiled it using GCC-4.8 with optimization option ‘-O3 -ffast-math’. HILUCSI has three key parameters, namely droptol (τ), condst (κ), and NNZ factor (α), for which we used 10^{-3} , 5, and 5, respectively, for all the tests. For ILU(0), we used MATLAB’s built-in ilu function with the “nofill” option; we chose this option because the more sophisticated ILUTP leads to superlinear complexity [21]. As can be seen from the table, HILUCSI outperformed ILU(0) by about a factor 8.2 and 12.9 on average in terms of the numbers of iterations for the level-1 and level-2 meshes, and by a factor of 2.7 and 4.3 on average in terms of solve times,

Table 5.3: Comparison of average number of GMRES iterations and solve times per time step between HILUCSI and ILU(0) for GL-3 with P_3 FEM for the AD equation with $\mathbf{v} = [10, 10, 10]^T$ and $\text{rtol} = 10^{-8}$. Times are in seconds. ‘-’ indicates non-convergence after 500 GMRES iterations. Leaders within each group are in boldface.

method	ILU	$\delta t = 1/4$				$\delta t = 1/16$				$\delta t = 1/64$			
		$\ell = 1$		$\ell = 2$		$\ell = 1$		$\ell = 2$		$\ell = 1$		$\ell = 2$	
		iter.	time	iter.	time	iter.	time	iter.	time	iter.	time	iter.	time
global	HILUCSI	5.4	0.41	9.2	8.13	4.9	0.38	8.3	7.33	3.2	0.22	5.8	4.49
	ILU(0)	45.2	0.76	115	18.8	41.9	0.85	92.1	15.2	23.4	0.44	54.7	9.14
BJF	HILUCSI	4.7	0.29	7.8	2.68	4.1	0.21	5.3	2.45	3.2	0.14	4.9	1.68
	ILU(0)	45.2	0.66	115	15.6	42.2	0.62	92.4	12.6	23.8	0.35	55.1	7.69
KPS	HILUCSI	12.8	0.34	14.6	3.38	12.3	0.3	13.1	3.25	10.1	0.22	10.4	2.4
	ILU(0)	83.3	0.71	223.6	21.3	54.2	0.47	128	12.2	26	0.25	57.4	6.06
BGS	HILUCSI	9.8	0.25	13.1	3.32	9.4	0.23	11.8	3.01	7.2	0.17	8	1.92
	ILU(0)	198.1	1.86	-	-	111.6	0.98	274	26.2	35.6	0.33	94.8	9.16

respectively. In addition, GMRES with ILU(0) failed to converge after 500 iterations for BGS on the level-2 mesh. We observed similar behavior for FDM. Hence, we will use HILUCSI in our later comparisons. In addition, it is worth noting that global and BJF preconditioners are comparable in terms of the number of iterations, but BJF is more efficient. Hence, it is desirable to consider block preconditioners rather than applying ILU on the global coefficient matrix. BJF outperformed KPS and BGS by more than a factor of two on average in terms of the number of iterations. Between BGS and KPS, they have better performance for smaller and larger $h^{-2}\delta t$, respectively, confirming our asymptotic analysis in Section 2.3.

Our previous timing results did not consider factorization cost. It is important to verify the near-linear complexity of its factorization and solve times. To this end, we solved the 3D AD equation under mesh refinement using FEM and FDM with the two-, three-, and four-stage GL schemes with $\delta t = 1/4$ but different orders of spatial accuracy. For simplicity, we only considered the PNKP in (2.4) to precondition GMRES. Figure 5.1 reports the factorization times and the averaged solve time per GMRES iteration at the first time step. These scalability tests were conducted on a Linux cluster with 2.5 GHz Intel(R) Xeon(R) E5-2680v3 processors and 64 GB of RAM. For accurate timing, both turbo and power-saving modes were turned off for the processors. It is clear that HILUCSI scaled (near) linearly in both factorization and solve times, confirming the analysis in [15]. Note that for P_2 FEM, the super-linear time complexity was due to the cache performance of the dense solve at the coarsest level in HILUCSI. It is also worth noting that the factorization cost is about an order of magnitude of that of solve times. The factorization is performed only at the first time step or when δt changes, so its cost can be amortized over many time steps. In our later analysis, we will only consider HILUCSI and we will focus on comparing the number of GMRES iterations. As a rule of thumb, the cost per GMRES iteration in BCSD, BJF, and BRSD is approximately twice as much as PNKP, and the cost of the others is comparable to PNKP.

5.2. Comparison of mathematically optimal preconditioners. We compare the mathematically optimal preconditioners, namely BCSD, BRSD, and BJF. As shown in Tables 5.3, BJF significantly outperformed KPS and BGS in terms of the number of GMRES iterations.

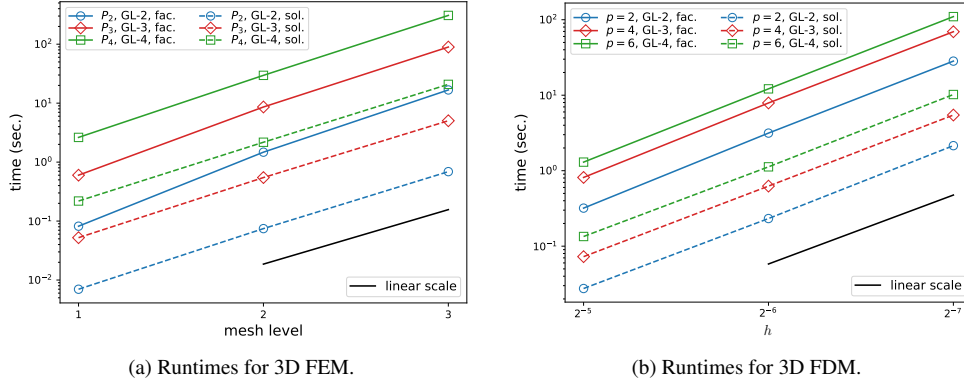


Figure 5.1: Factorization and solve times of PNKP for 3D FEM (left) and FDM (right). Solid and dashed lines are for the factorization times of HILUCSI and averaged solve times per GMRES iteration, respectively.

Hence, it suffices to compare BCSD and BRSD with BJF. In addition, since PNKP is optimal as $h^{-2}\delta t \rightarrow \infty$, we also include it as a point of reference due to its simplicity.

As in Section 5.1, we discretized the 3D AD equation (1.1) using both FEM and FDM with different velocities. For FEM, we used the two- and three-stage GL schemes (i.e., GL-2 and GL-3, respectively), which converge at the rates of $\mathcal{O}(\delta t^4)$ and $\mathcal{O}(\delta t^6)$ in time, correspondingly. For GL-2 and GL-3, we used P_2 and P_3 elements for spatial discretization, correspondingly, where P_k FEM converges at $\mathcal{O}(h^{k+1})$ in L^2 norm. We used $\text{rtol} = 10^{-6}$ and 10^{-10} as the convergence tolerance in GMRES for GL-2 and GL-3, respectively. Table 5.4 shows the average numbers of GMRES iterations. It is worth noting that BCSD and BJF had comparable performance, and they both significantly outperformed PNKP on coarser meshes, although PNKP is quite competitive with larger time steps on the finest mesh. BRSD performed slightly worse than BCSD and BJF because its larger $2m \times 2m$ diagonal blocks tend to introduce more droppings.

For FDM, we used second- and sixth-order finite differences (i.e., $p = 2$ and $p = 6$, respectively) in space, and used the GL-2 and GL-4 in time, correspondingly. Table 5.5 shows the average numbers of GMRES iterations. Similar to the FEM results, BCSD and BJF are mostly comparable, but BCSD outperformed BJF on average. BRSD performed slightly worse than BCSD and BJF. PNKP performed the worse overall, by up to a factor of eight in one case. Hence, the more sophisticated manipulations in BCSD, BJF, and BCSD are beneficial in general, compared to the simple PNKP.

5.3. Effect of ordering in CSD and RSD. In this work, we suggest to order the diagonal blocks in BCSD (and SABRSD) based on the ascending order of $|d_i|$, due to Proposition 3.5 and an assumption of insensitivity of $\|\delta \mathbf{D}_j \mathbf{x}_j\|$ and $\|\mathbf{R}_{ij}\|$ to ordering. This analysis and assumption require some numerical verification to demonstrate the potential benefits. Table 5.6 compares the average numbers of GMRES iterations for the GL-5 and GL-6 with sixth-order finite difference method for the 3D AD equation. We ordered the diagonal entries in CSD in ascending and descending orders of $|d_i|$ for BCSD and BCSD-R, respectively; similarly for SABRSD and SABRSD-R. It can be seen that BCSD and SABRSD outperformed BCSD-R and SABRSD-R, respectively. The benefit for SABRSD is particularly significant, with a margin of about 30% on average. Furthermore, SABRSD-R for GL-5 did not reach the

Table 5.4: Comparison of the average numbers of GMRES iterations preconditioned by BCSD, BRSD, BRSD, and PNKP for GL-2 and GL-3 with P_2 and P_3 FEM for the AD equation with $\mathbf{v} = [10, 10, 10]^T$ and $\text{rtol} = 10^{-6}$ and 10^{-8} , respectively. Numbers in parentheses indicate the number of stages. The leaders are in boldface.

method	$\delta t = 1/4$			$\delta t = 1/16$			$\delta t = 1/64$		
	$\ell = 1$	2	3	$\ell = 1$	2	3	$\ell = 1$	2	3
BCSD(2)	4	6	10.3	4	5.3	9.2	3	4	6
BJF(2)	4.2	5.9	10.1	4	5.3	9.1	3	4	6.8
BRSD(2)	4	6.4	11.9	3.3	6.0	10.8	2.4	3.9	7.1
PNKP(2)	6.2	6.4	11.6	9.0	8.7	10.4	12.0	12.2	9.4
BCSD(3)	4.8	7.9	16.3	4.1	6.7	12.8	3	4.6	7.3
BJF(3)	4.7	7.8	14.7	4.1	7.1	13.1	3.2	4.9	8.8
BRSD(3)	5.2	9.1	17.7	4.9	8.0	15.0	3.1	5.0	9.8
PNKP(3)	9.3	8.9	15.0	14.6	13.8	14.6	24.0	23.1	18.3

Table 5.5: Comparison of the average numbers of GMRES iterations preconditioned by BCSD, BRSD, BRSD, and PNKP for GL-2 and GL-4 with FDM for the AD equation with $\mathbf{v} = [1, 1, 1]^T$ and $\text{rtol} = 10^{-6}$ and 10^{-10} , respectively. Numbers in parentheses indicate the number of stages. The leaders in each group are in boldface.

method	$\delta t = 1/4$			$\delta t = 1/16$			$\delta t = 1/64$		
	$h = 1/32$	$1/64$	$1/128$	$h = 1/32$	$1/64$	$1/128$	$h = 1/32$	$1/64$	$1/128$
BCSD(2)	12	23.9	55.1	9.2	17.1	33.9	4.8	8.4	15.9
BJF(2)	12.1	23.2	55.1	9.7	18.1	37.2	5.6	9.7	18.6
BRSD(2)	11.8	22.2	49.8	9.4	17.4	34.0	5.6	9.7	18.2
PNKP(2)	12.0	23.2	55.1	9.9	18.7	37.3	9.0	10.4	18.9
BCSD(4)	13.6	27.2	62.8	9.1	17.3	35.9	5.9	9.3	18.4
BJF(4)	13.6	25.8	59.9	10.7	20.3	43.9	6.7	11.4	22.6
BRSD(4)	13.0	25.1	58.1	10.3	19.4	40.3	6.6	11.2	21.7
PNKP(4)	15.8	26.8	61.3	24.4	23.6	47.0	49.4	28.7	26.9

10^{-12} relative tolerance and stagnated at about 10^{-11} . We note that for GL-3 and GL-4, the ordering also led to a difference with similar margins for SABRSD, but its effect on BCSD was not pronounced.

As a side product, Table 5.6 also shows that the number of GMRES iterations of BCSD is about 60% of that of SABRSD on average. Since BCSD (and similar BRSD) is approximately twice as expensive as SABRSD per GMRES iteration, SABRSD is competitive as a limited-memory, near-optimal preconditioner.

5.4. Effect of optimization in SABRSD. Finally, we demonstrate the effectiveness of the optimization techniques of SABRSD in Section 4.1. To this end, we compare SABRSD with TBRSD, which simply truncates the lower-triangular part of the sorted and permuted \mathbf{R} matrix in RSD. Table 5.7 shows the average numbers of GMRES iterations for GL-3 and GL-4 with P_3 and P_4 finite element methods, respectively, for the 3D AD equation. It can

Table 5.6: Assessment of the impact of ordering on BCSD and SABRSD on the average numbers of GMRES iterations for the GL-5 and GL-6 with sixth-order FDM for the AD equation with $v = [1, 1, 1]^T$ and $\text{rtol} = 10^{-12}$. The numbers in the parentheses indicate the number of stages. ‘-’ indicates stagnation. The leaders in each group are in boldface.

method	$\delta t = 1/4$			$\delta t = 1/16$			$\delta t = 1/64$		
	$h = 1/32$	$1/64$	$1/128$	$h = 1/32$	$1/64$	$1/128$	$h = 1/32$	$1/64$	$1/128$
BCSD(5)	15.8	32.3	77.2	11	20.6	44.8	7	10.9	22.2
BCSD-R(5)	15.8	30.9	82.9	11.2	22.3	49.4	6.9	11.7	24
SABRSD(5)	23.7	56.9	171.6	18.9	26.0	63.9	17.1	17.4	23.4
SABRSD-R(5)	33.8	75.7	–	28.1	36.4	79.8	25.1	25.4	32.2
BCSD(6)	15.7	32.8	80	11	20.6	46.9	6.7	10.9	21.6
BCSD-R(6)	15.8	33	84.8	11	22	50.8	6.1	11.3	23
SABRSD(6)	25.7	58.0	168.8	22.7	26.1	61.8	21.4	20.4	23.4
SABRSD-R(6)	35.9	76.4	209.4	32.8	36.9	77.8	29.4	29.3	33.2

be seen that SABRSD always outperformed TBRSD, and it reduced the number of GMRES iterations by about 20% on average. As a point of reference, we also compared SABRSD with SOBT, which applies the optimization strategy on the transpose of the Butcher array. Our results show that SOBT improved over BGS up to about 10% on finer meshes for GL-3, but it did not improve for GL-4. These results indicate that our asymptotic analysis in Section 4.1 works well only when $h^{-2}\delta t$ is sufficiently large, and the optimization works the best when combined with the ordering described in Section 4.2. As a cross reference with existing methods, Table 5.7 also included the number of GMRES iterations of KPS [13]. It can be seen that SABRSD outperformed BGS and KPS by 17% and 32% on average, respectively, although it slightly under-performed KPS in two cases with the largest δt on the finest mesh.

6. Conclusion. We introduced three mathematically optimal preconditioners (namely *BRCD*, *BRSD*, and *BJF*) and a limited-memory near-optimal preconditioner *SABRSD*, for fully implicit RK schemes in solving parabolic PDEs. The optimal preconditioners have high memory requirements and factorization costs. In comparison, *SABRSD* has a comparable memory requirement and factorization cost as a singly diagonally implicit RK scheme (SDIRK). We optimized *SABRSD* based on the mathematical theory of ϵ -accurate preconditioners. We approximately factorized the diagonal blocks in these preconditioners using near-linear complexity ILU factorizations, including HILUCSI and ILU(0). Our numerical results showed that HILUCSI is significantly more robust and more efficient than using ILU(0). With HILUCSI, we then showed that BCSD and BRSD significantly outperformed the prior state-of-the-art block preconditioners in terms of the number of GMRES iterations. *SABRSD* outperformed the prior state-of-the-art block preconditioners (namely, BGS and KPS) by 17–32% on average. *SABRSD* also compared reasonably well with BCSD in terms of the computational cost while requiring much less memory.

This work primarily focused on the Gauss-Legendre schemes for their optimal accuracy. However, our techniques can be generalized to other A-stable FIRK (such as Radau IIA and Lobatto IIIC) and DIRK schemes to develop low-memory, near-optimal block preconditioners. While *SABRSD* minimizes memory usage compared to BCSD and BRSD, it

Table 5.7: Comparison of the effect of singly-diagonal optimization for the average numbers of GMRES iterations for GL-3 and GL-4 with P_3 and P_4 FEM for AD equation with $\mathbf{v} = [10, 10, 10]^T$ and $\text{rtol} = 10^{-2s-2}$, respectively. The numbers in the parentheses indicate the number of stages. The leaders in each group are in boldface.

method	$\delta t = 1/4$			$\delta t = 1/16$			$\delta t = 1/64$		
	$\ell = 1$	2	3	$\ell = 1$	2	3	$\ell = 1$	2	3
SABRSD(3)	8.4	11.4	22.8	8.3	8.8	16.4	6.9	6.9	7.8
TBRSD(3)	9.8	13.4	24.8	10.7	12.6	19.8	8.0	8.7	11.3
SOBT(3)	11.0	13.6	25.0	10.7	11.3	18.4	8.6	8.8	9.8
BGS(3)	9.8	13.1	25.4	9.4	11.8	19.6	7.2	8.0	11.2
KPS(3)	12.8	14.6	22.7	12.3	13.1	17.7	10.1	10.4	12.2
SABRSD(4)	13.2	15.6	32.9	13.3	13.3	20.6	11.3	11.7	11.7
TBRSD(4)	16.0	20.6	41.3	16.7	19.2	28.3	13.3	13.9	17.0
SOBT(4)	19.6	22.6	45.0	19.9	20.7	27.3	16.0	16.4	17.1
BGS(4)	15.4	19.1	43.4	15.1	17.6	28.2	11.6	12.6	16.9
KPS(4)	18.1	20.0	30.4	17.3	17.8	22.6	14.7	15.4	17.3

is worth developing flexible variants with different diagonal entries, which require generalizing the error analysis and the optimization strategies developed in this work. Other future research directions include hybridizing the optimal preconditioners and comparing SABRSD-preconditioned FIRK and DIRK schemes in terms of accuracy and efficiency.

Acknowledgments. The authors thank the support of the CANGA project under the Scientific Discovery through Advanced Computing (SciDAC) program in the US Department of Energy’s Office of Science, Office of Advanced Scientific Computing Research through subcontract #462974 with Los Alamos National Laboratory. Computational results were obtained using the Seawulf cluster at the Institute for Advanced Computational Science of Stony Brook University, which was partially funded by the Empire State Development grant NYS #28451.

REFERENCES

- [1] M. ALNÆS, J. BLECHTA, J. HAKE, A. JOHANSSON, B. KEHLET, A. LOGG, C. RICHARDSON, J. RING, M. E. ROGNES, AND G. N. WELLS, *The FEniCS project version 1.5*, Arch. Numer. Sofw., 3 (2015).
- [2] P. R. AMESTOY, T. A. DAVIS, AND I. S. DUFF, *An approximate minimum degree ordering algorithm*, SIAM J. Matrix Anal. Appl., 17 (1996), pp. 886–905.
- [3] M. BENZI, *Preconditioning techniques for large linear systems: a survey*, J. Comput. Phys., 182 (2002), pp. 418–477.
- [4] D. BERTACCINI, *A circulant preconditioner for the systems of LMF-based ODE codes*, SIAM J. Sci. Comput., 22 (2000), pp. 767–786.
- [5] T. A. BICKART, *An efficient solution process for implicit Runge–Kutta methods*, SIAM J. Numer. Anal., 14 (1977), pp. 1022–1027.
- [6] M. BOLLHÖFER, J. I. ALIAGA, A. F. MARTÍN, AND E. S. QUINTANA-ORTÍ, *ILUPACK*, Encyclopedia of Parallel Computing, (2011), pp. 917–926.
- [7] M. BOLLHÖFER AND Y. SAAD, *Multilevel preconditioners constructed from inverse-based ILUs*, SIAM J. Sci. Comput., 27 (2006), pp. 1627–1650.
- [8] J. H. BRANDTS, *MATLAB code for sorting real Schur forms*, Numer. Linear Algebra Appl., 9 (2002), pp. 249–261.
- [9] J. C. BUTCHER, *On the implementation of implicit Runge-Kutta methods*, BIT Numer. Math., 16 (1976), pp. 237–240.

- [10] J. C. BUTCHER, *Numerical Methods for Ordinary Differential Equations*, Wiley, third ed., 2016.
- [11] R. H. CHAN, M. K. NG, AND X.-Q. JIN, *Strang-type preconditioners for systems of LMF-based ODE codes*, IMA J. Numer. Anal., 21 (2001), pp. 451–462.
- [12] T. F. CHAN, *An optimal circulant preconditioner for Toeplitz systems*, SIAM J. Sci. Stat. Comput., 9 (1988), pp. 766–771.
- [13] H. CHEN, *A splitting preconditioner for the iterative solution of implicit Runge-Kutta and boundary value methods*, BIT Numer. Math., 54 (2014), pp. 607–621.
- [14] H. CHEN, *Generalized Kronecker product splitting iteration for the solution of implicit Runge-Kutta and boundary value methods*, Numer. Linear Algebra Appl., 22 (2015), pp. 357–370.
- [15] Q. CHEN, A. GHAI, AND X. JIAO, *HILUCSI: Simple, robust, and fast multilevel ILU for large-scale saddle-point problems from PDEs*, arXiv preprint, (2019), <https://arxiv.org/abs/1911.10139>.
- [16] R. CONLEY, T. J. DELANEY, AND X. JIAO, *A hybrid method and unified analysis of generalized finite differences and lagrange finite elements*, J. Comput. Appl. Math., (2020), p. 112862.
- [17] G. G. DAHLQUIST, *A special stability problem for linear multistep methods*, BIT Numer. Math., 3 (1963), pp. 27–43.
- [18] J. DONEA AND A. HUERTA, *Finite element methods for flow problems*, John Wiley & Sons, 2003.
- [19] I. S. DUFF AND J. KOSTER, *On algorithms for permuting large entries to the diagonal of a sparse matrix*, SIAM J. Matrix Anal. Appl., 22 (2001), pp. 973–996.
- [20] A. ERN AND J.-L. GUERMOND, *Theory and Practice of Finite Elements*, vol. 159, Springer Science & Business Media, 2013.
- [21] A. GHAI, C. LU, AND X. JIAO, *A comparison of preconditioned Krylov subspace methods for large-scale nonsymmetric linear systems*, Numer. Linear Algebra Appl., 26 (2017), p. e2215.
- [22] G. H. GOLUB AND C. F. VAN LOAN, *Matrix Computations*, Johns Hopkins, 4th ed., 2013.
- [23] E. HAIRER AND G. WANNER, *Solving Ordinary Differential Equations II: Stiff and Differential-Algebraic Problems*, Springer Berlin Heidelberg, second revised ed., 1996.
- [24] W. HUANG, L. KAMENSKI, AND J. LANG, *Conditioning of implicit Runge-Kutta integration for finite element approximation of linear diffusion equations on anisotropic meshes*, J. Comput. Appl. Math., (2019), p. 112497.
- [25] A. ISERLES, *A First Course in the Numerical Analysis of Differential Equations*, Cambridge University Press, second ed., 2009.
- [26] A. JAMESON, *Evaluation of fully implicit Runge Kutta schemes for unsteady flow calculations*, J. Sci. Comput., 73 (2017), pp. 819–852.
- [27] X. JIAO AND Q. CHEN, *Approximate generalized inverses with iterative refinement for ϵ -accurate preconditioning of singular systems*, arxiv, (2020). arXiv:2009.01673.
- [28] B. S. JOVANOVIĆ AND E. SÜLI, *Analysis of finite difference schemes: for linear partial differential equations with generalized solutions*, vol. 46, Springer Science & Business Media, 2013.
- [29] A. KANEVSKY, M. H. CARPENTER, D. GOTTLIEB, AND J. S. HESTHAVEN, *Application of implicit-explicit high order Runge-Kutta methods to discontinuous-Galerkin schemes*, J. Comput. Phys., 225 (2007), pp. 1753–1781.
- [30] G. KARNIADAKIS AND S. SHERWIN, *Spectral/hp element methods for computational fluid dynamics*, Oxford University Press, second ed., 2005.
- [31] R. J. LEVEQUE, *Finite Difference Methods for Ordinary and Partial Differential Equations: Steady-State and Time-Dependent Problems*, SIAM, 2007.
- [32] A. LOGG, K.-A. MARDAL, AND G. WELLS, *Automated Solution of Differential Equations by The Finite Element Method: The FEniCS Book*, vol. 84, Springer Science & Business Media, 2012.
- [33] K.-A. MARDAL, T. K. NILSSEN, AND G. A. STAFF, *Order-optimal preconditioners for implicit Runge-Kutta schemes applied to parabolic PDEs*, SIAM J. Sci. Comput., 29 (2007), pp. 361–375.
- [34] J. MAYER, *A multilevel Crout ILU preconditioner with pivoting and row permutation*, Numer. Linear Algebra Appl., 14 (2007), pp. 771–789.
- [35] A. NAJAFI-YAZDI AND L. MONGEAU, *A low-dispersion and low-dissipation implicit Runge-Kutta scheme*, J. Comput. Phys., 233 (2013), pp. 315–323.
- [36] W. PAZNER AND P.-O. PERSSON, *Stage-parallel fully implicit Runge-Kutta solvers for discontinuous Galerkin fluid simulations*, J. Comput. Phys., 335 (2017), pp. 700–717.
- [37] P.-O. PERSSON, *Scalable parallel Newton-Krylov solvers for discontinuous Galerkin discretizations*, in 47th AIAA Aerospace Sciences Meeting Including The New Horizons Forum and Aerospace Exposition, 2009, p. 606.
- [38] Y. SAAD, *Preconditioning techniques for nonsymmetric and indefinite linear systems*, J. Comput. Appl. Math., 24 (1988), pp. 89–105.
- [39] Y. SAAD, *A flexible inner-outer preconditioned GMRES algorithm*, SIAM J. Sci. Comput., 14 (1993), pp. 461–469.
- [40] Y. SAAD, *ILUT: A dual threshold incomplete LU factorization*, Numer. Linear Algebra Appl., 1 (1994), pp. 387–402.

- [41] Y. SAAD, *Iterative Methods for Sparse Linear Systems*, SIAM, 2nd ed., 2003.
- [42] Y. SAAD, *Multilevel ILU with reorderings for diagonal dominance*, SIAM J. Sci. Comput., 27 (2005), pp. 1032–1057.
- [43] Y. SAAD AND M. H. SCHULTZ, *GMRES: A generalized minimal residual algorithm for solving nonsymmetric linear systems*, SIAM J. Sci. Stat. Comput., 7 (1986), pp. 856–869.
- [44] G. A. STAFF, K.-A. MARDAL, AND T. K. NILSSEN, *Preconditioning of fully implicit Runge-Kutta schemes for parabolic PDEs*, Model. Ident. Control, 27 (2006), pp. 109–123.
- [45] THE MATHWORKS, INC., *MATLAB R2020b*. Natick, MA, 2020.
- [46] L. N. TREFETHEN AND D. BAU III, *Numerical Linear Algebra*, vol. 50, SIAM, 1997.
- [47] E. E. TYRTYSHNIKOV, *Optimal and superoptimal circulant preconditioners*, SIAM J. Matrix Anal. Appl., 13 (1992), pp. 459–473.
- [48] P. VAN DER HOUWEN AND J. DE SWART, *Triangularly implicit iteration methods for ODE-IVP solvers*, SIAM J. Sci. Comput., 18 (1997), pp. 41–55.
- [49] C. ZHANG, H. CHEN, AND L. WANG, *Strang-type preconditioners applied to ordinary and neutral differential-algebraic equations*, Numer. Linear Algebra Appl., 18 (2011), pp. 843–855.

Appendix A. Sorting and Permuting RSD. Real Schur decomposition is not unique, and BRSD and SABRSD use different orderings and permutations of the diagonal blocks. To sort RSD, we use the SRSchur function in [8], except that we need to replace its select sub-function to sort by the real part of the diagonal blocks. In terms of the orientation, let \mathbf{R}_i denote a 2-by-2 diagonal block in \mathbf{R}_* from the sorted RSD $\mathbf{A} = \mathbf{Q}_* \mathbf{R}_* \mathbf{Q}_*^T$, and let \mathbf{S}_i be its corresponding 2×2 permutation matrix. Let \mathbf{P}_i denote the $s \times s$ permutation matrix

$$\mathbf{P}_i = \begin{bmatrix} \mathbf{I}_{s_1} & & \\ & \mathbf{S}_i & \\ & & \mathbf{I}_{s_2} \end{bmatrix},$$

where s_1 and s_2 are the numbers of rows above and below \mathbf{R}_i , respectively. The sorted and permuted RSD is then

$$(A.1) \quad \mathbf{A} = \mathbf{Q} \mathbf{R} \mathbf{Q}^T, \text{ where } \mathbf{R} = \mathbf{P}_{\lceil s/2 \rceil} \cdots \mathbf{P}_1 \mathbf{R}_* \mathbf{P}_1^T \cdots \mathbf{P}_{\lceil s/2 \rceil}^T \text{ and } \mathbf{Q} = \mathbf{Q}_* \mathbf{P}_1^T \cdots \mathbf{P}_{\lceil s/2 \rceil}^T.$$

Appendix B. Optimization for SABRSD. In SABRSD, we minimize $\|\mathbf{I} - \mathbf{R}\hat{\mathbf{R}}^{-1}\|$ subjective to $\min \kappa(\mathbf{R}\hat{\mathbf{R}}^{-1})$. This optimization is highly nonlinear, and we solved it using the fmincon function in MATLAB’s Global Optimization Toolbox [45]. For the s -stage GL scheme, $\hat{\mathbf{R}}$ has $s(s-1)/2$ variables for the strictly upper-triangular part and one variable in the diagonal. Since $\kappa(\mathbf{R}\hat{\mathbf{R}}^{-1})$ is invariant of scaling of $\hat{\mathbf{R}}$, we perform the optimization in two steps. First, we solved for $\hat{\mathbf{R}}_* = \arg \min_{\hat{\mathbf{R}}} \kappa(\mathbf{R}\hat{\mathbf{R}}^{-1})$ while fixing the diagonal entries to be 1. In the second step, we solve for a scalar factor $\alpha \in (0, 1]$ by minimizing $\|\mathbf{I} - \mathbf{R}(\alpha \hat{\mathbf{R}}_*)^{-1}\| = \|\mathbf{I} - \frac{1}{\alpha} \mathbf{R}\hat{\mathbf{R}}_*^{-1}\|$ for $\hat{\mathbf{R}}_*$ obtained from the first step. For both steps, we use 10^{-12} as the relative convergence tolerances by default, but a larger threshold (e.g., 10^{-8}) may also suffice. We verified the procedure for the GL schemes with up to 11 stages.